

# MIMO Space-Time Block Coding (STBC): Simulations and Results

Luis Miguel Cortés-Peña

**Abstract**—Wireless networks have quickly become part of everyday life. Wireless LANs, cell phone networks, and personal area networks are just a few examples of widely used wireless networks. However, wireless devices are range and data rate limited. The research community has spent a great deal of effort on finding ways to overcome these limitations. One method is to use Multiple-Input Multiple-Output (MIMO) links. The multiple antennas allow MIMO systems to perform precoding (multi-layer beamforming), diversity coding (space-time coding), and spatial multiplexing. Beamforming consists of transmitting the same signal with different gain and phase (called weights) over all transmit antennas such that the receiver signal is maximized. Diversity consists of transmitting a single space-time coded stream through all antennas. Spatial multiplexing increases network capacity by splitting a high rate signal into multiple lower rate streams and transmitting them through the different antennas. In spatial multiplexing, the receiver can successfully decode each stream given that the received signals have sufficient spatial signatures and that the receiver has enough antennas to separate the streams. The result of using these MIMO techniques is higher data rate or longer transmit range without requiring additional bandwidth or transmit power. This paper presents a detailed study of diversity coding for MIMO systems. Different space-time block coding (STBC) schemes including Alamouti's STBC for 2 transmit antennas as well as orthogonal STBC for 3 and 4 transmit antennas are explored. Finally, these STBC techniques are implemented in MATLAB and analyzed for performance according to their bit-error rates using BPSK, QPSK, 16-QAM, and 64-QAM modulation schemes.

**Index Terms**—Personal & Mobile Communications; ECE 6604; Space Time Block Coding; STBC; Computer Simulation; OSTBC; Orthogonal Space-Time Coding; MIMO; Multiple-Input Multiple-Output (MIMO) Systems; Georgia Tech;

## I. INTRODUCTION

IT has come a long way since Tesla, using Maxwell and Hertz's work on transmission of electromagnetic waves, demonstrated the transmission of information through a wireless medium using such waves [1]. The Second World War led to much interest in this area, giving way to many of the theoretical foundations of communications. Claude Shannon's work in 1948, which provided an upper bound to the error-free data rate under the signal-to-noise ratio (SNR) constraint, appeared during that time. Wireless networks widely used today include: cellular networks, wireless mesh networks (WMNs), wireless Local Area Networks (WLANs), personal area networks (PANs), and wireless sensor networks (WSNs). The increasing demand for these networks has turned spectrum into a precious resource. For this reason, there is always a need for methods to pack more bits per Hz. A particular solution that has caught researcher's attention is the use of multiple antennas at both transmitter (TX) and receiver (RX). The use

of MIMO for increasing capacity dates back to Winters in [2]. Such a system is called a Multiple-Input Multiple-Output (MIMO) system. Advantages of MIMO systems include [1], [3]:

- *Beamforming* - A transmitter receiver pair can perform beamforming and direct their main beams at each other, thereby increasing the receiver's received power and consequently the SNR.
- *Spatial diversity* - A signal can be coded through the transmit antennas, creating redundancy, which reduces the outage probability.
- *Spatial multiplexing* - A set of streams can be transmitted in parallel, each using a different transmit antenna element. The receiver can then perform the appropriate signal processing to separate the signals.

It is important to note that each antenna element on a MIMO system operates on the same frequency and therefore does not require extra bandwidth. Also, for fair comparison, the total power through all antenna elements is less than or equal to that of a single antenna system, i.e.

$$\sum_{k=1}^N p_k \leq P \quad (1)$$

where  $N$  is the total number of antenna elements,  $p_k$  is the power allocated through the  $k^{\text{th}}$  antenna element, and  $P$  is the power if the system had a single antenna element [4]. Effectively, (1) ensures that a MIMO system consumes no extra power due to its multiple antenna elements.

As a consequence of their advantages, MIMO wireless systems have captured the attention of international standard organizations. The use of MIMO has been proposed multiple times for use in the high-speed packet data mode of third-generation cellular systems (3G) [1], [3] as well as the fourth-generation cellular systems (4G) [5], [6], [7]. MIMO has also influenced wireless local area networks (WLANs) as the IEEE 802.11n standard exploits the use of MIMO systems to acquire throughputs as high as 600Mbps [8], [9].

This paper provides a brief background on MIMO systems including the system model, capacity analysis, and channel models. Focus is then given to spatial diversity, specifically to space time block codes (STBC). We discuss Alamouti's STBC as well as other orthogonal STBC for 3 and 4 transmit antennas and finally show simulation results and analysis.

The paper is organized as follows. In Section II, important general background information on MIMO is provided. Next, different STBC techniques are explained in Section III. The simulation methodology is discussed in Section IV. Results

and analysis are presented in Section V. Finally, Section VI concludes this paper.

## II. BACKGROUND

Traditional wireless systems are affected by multipath propagation. In MIMO systems, however, this multipath effect is exploited to benefit the user. In fact, the separability of parallel streams depend on the presence of rich multipath. The reason for this effect will become apparent as the System Model is described in Section II-A below.

### A. System Model

MIMO systems are composed of three main elements, namely the transmitter (TX), the channel ( $\mathbf{H}$ ), and the receiver (RX). In this paper,  $N_t$  is denoted as the number of antenna elements at the transmitter, and  $N_r$  is denoted as the number of elements at the receiver. Figure 1 depicts such MIMO system block diagram. It is worth noting that system is described in terms of the channel. For example, the Multiple-Inputs are located at the output of the TX (the input to the channel), and similarly, the Multiple-Outputs are located at the input of the RX (the output of the channel).

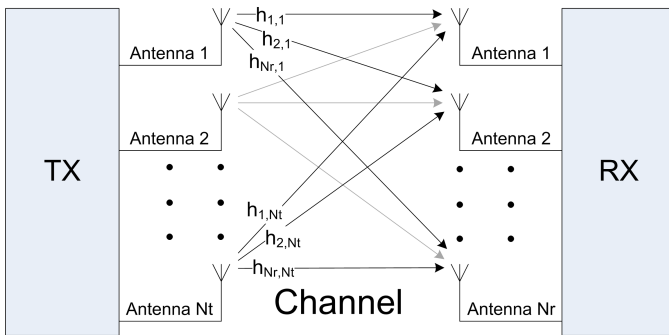


Fig. 1. Multiple-Input Multiple-Output system block diagram.

The channel with  $N_r$  outputs and  $N_t$  inputs is denoted as a  $N_r \times N_t$  matrix:

$$\mathbf{H} = \begin{pmatrix} h_{1,1} & h_{1,2} & \cdots & h_{1,N_t} \\ h_{2,1} & h_{2,2} & \cdots & h_{2,N_t} \\ \vdots & \vdots & \ddots & \vdots \\ h_{N_r,1} & h_{N_r,2} & \cdots & h_{N_r,N_t} \end{pmatrix} \quad (2)$$

where each entry  $h_{i,j}$  denotes the attenuation and phase shift (transfer function) between the  $j^{th}$  transmitter and the  $i^{th}$  receiver. It is assumed throughout this paper that the MIMO channel behaves in a “quasi-static” fashion, i.e. the channel varies randomly between burst to burst, but fixed within a transmission. This is a reasonable and commonly used assumption as it represents an indoor channel where the time of change is constant and negligible compared to the time of a burst of data [10].

The MIMO signal model is described as

$$\vec{r} = \mathbf{H}\vec{s} + \vec{n} \quad (3)$$

where  $\vec{r}$  is the received vector of size  $N_r \times 1$ ,  $\mathbf{H}$  is the channel matrix of size  $N_r \times N_t$ ,  $\vec{s}$  is the transmitted vector of size  $N_t \times 1$ , and  $\vec{n}$  is the noise vector of size  $N_r \times 1$ . Each noise element is typically modeled as independent identically distributed (i.i.d.) white Gaussian noise [1], [4] with variance  $N_t/(2 \cdot SNR)$  [11]. An explanation for this model is as follows. The transmitted signals are mixed in the channel since they use the same carrier frequency. At the receiver side, the received signal is composed of a linear combination of each transmitted signal plus noise. The receiver can solve for the transmitted signals by treating (3) as a system of linear equations [3]. If the channel  $\mathbf{H}$  is correlated, the system of linear equations will have more unknowns than equations. One reason correlation between signals can occur is due to the spacing between antennas. To prevent correlation due to the spacing, they are typically spaced at least  $\lambda_c/2$ , where  $\lambda_c$  is the wavelength of the carrier frequency [1]. The second reason correlation can occur is due to lack of multipath components. It is for this reason that rich multipath is desirable in MIMO systems. The multipath effect can be interpreted by each receive antenna being in a different channel. For this reason, the *rank* of a MIMO channel is defined as the number of independent equations offered. It is important to note that

$$\text{rank}(\mathbf{H}) \leq \min(N_r, N_t) \quad (4)$$

and therefore the maximum number of streams that a MIMO system can support is upper-bounded by  $\min(N_r, N_t)$ .

Since the performance of MIMO systems depends highly on the channel matrix, it is important to model the channel matrix realistically. The following section provides an overview of typical channel models used for computer simulations.

### B. Channel Models

Channel models for MIMO systems can be either simple or very complex, depending on the environment modeled and the desired accuracy. There are two different techniques for modeling MIMO channels. One method is to calculate the MIMO channel matrix according to a physical representation of the environment. The channel matrix in such a physical model would depend on physical parameters such as the angle of arrival (AOA), angle of departure (AOD), and time of arrival (TOA) [12]. In [13], Molisch presents a physical MIMO model and provides typical physical parameters for both macro and microcell environments. As expected, these type of deterministic models are highly complex. Another technique to model MIMO channels, is to model the channel analytically. Such a model treats all channels between each transmit antenna to each receive antenna as SISO channels. This type of model assumes that the channels are independent and identically distributed (i.i.d.). However, depending on the environment modeled, this assumption is rarely true. The reason is that MIMO channels can experience spatial correlation between links [12]. It is possible to generate a MIMO channel with a specific correlation matrix. The channel correlation matrix is usually measured in the field and it is tied to the environment setup such as antenna element patterns, spacing between antennas, and surrounding reflectors [12]. Since one

of the main goals of this paper is to compare the performance of different STBC schemes, the channel model is chosen such that the correlation does not interfere with the performance of such. Next, two channel models are discussed for the case of non-line-of-sight (NLOS) and the case of line-of-sight (LOS) respectively.

1) *NLOS Environment*: A typical model used in research to model NLOS scenarios is the Rayleigh model. The Rayleigh model assumes NLOS, and is used for environments with a large number of scatterers. The Rayleigh model has independent identically distributed (i.i.d.) complex, zero mean, unit variance channel elements and is given by [10]:

$$h_{ij} = \frac{1}{\sqrt{2}} \left( \text{Normal}(0, 1) + \sqrt{-1} \cdot \text{Normal}(0, 1) \right) \quad (5)$$

This model results in an approximation which improves as the spacing between antennas become large compared to the wavelength  $\lambda$ .

2) *LOS Model*: The MIMO channel matrix for the LOS scenario is given by [12]:

$$\mathbf{H} = \sqrt{\frac{K}{1+K}} \mathbf{H}_{LOS} + \sqrt{\frac{1}{1+K}} \mathbf{H}_{NLOS} \quad (6)$$

where:

$$K(\text{dB}) = 10 \log_{10} \frac{P_{LOS}}{P_{NLOS}} \quad (7)$$

In (6),  $\mathbf{H}_{LOS}$  is a rank-one matrix corresponding to the LOS component, and the  $\mathbf{H}_{NLOS}$  corresponds to the NLOS components. In (7),  $P_{LOS}$  is the power due to the LOS component, and  $P_{NLOS}$  is due to the power of the NLOS component [12]. The  $\mathbf{H}_{NLOS}$  component is usually modeled as (5) [3]. In SISO systems, the higher the  $K$  factor, the smaller the fade margin needed. For MIMO systems, the higher the  $K$  factor, the more dominant the rank-one  $\mathbf{H}_{LOS}$  component will be, and consequently, the less dominant the  $\mathbf{H}_{NLOS}$  component will be. However, for the scenario of rich multipath, simulations and measurements have shown that the LOS component rarely dominates [3].

### III. SPACE-TIME BLOCK CODING

One of the methodologies for exploiting the capacity in MIMO system consists of using the additional diversity of MIMO systems, namely spatial diversity, to combat channel fading. This can be achieved by transmitting several replicas of the same information through each antenna. By doing this, the probability of losing the information decreases exponentially [3]. The antennas in a MIMO system are used for supporting a transmission of a SISO system since the targeted rate of is that of a SISO system. The *diversity order* or *diversity gain* of a MIMO system is defined as the number of independent receptions of the same signal. A MIMO system with  $N_t$  transmit antennas and  $N_r$  receive antennas has potentially *full diversity* (i.e. maximum diversity) gain equal to  $N_t N_r$ .

The different replicas sent for exploiting diversity are generated by a space-time encoder which encodes a single stream through space using all the transmit antennas and through time by sending each symbol at different times. This form of coding is called Space-Time Coding (STC). Due to

their decoding simplicity, the most dominant form of STCs are space-time block codes (STBC). In the next sections, we discuss different STBC techniques which will be then compared for performance in Section V.

#### A. Alamouti's STBC

In [14], Alamouti published his technique on transmit diversity. Historically, Alamouti's scheme was the first STBC [4]. The simplicity and structure of the Alamouti STBC has placed the scheme in both the W-CDMA and CDMA-2000 standards [3]. The Alamouti STBC scheme uses two transmit antennas and  $N_r$  receive antennas and can accomplish a maximum diversity order of  $2N_r$  [14]. Moreover, the Alamouti scheme has *full rate* (i.e. a rate of 1) since it transmits 2 symbols every 2 time intervals. Next, a description of the Alamouti scheme is provided for both 1 and 2 receive antennas, followed by a general expression for the decoding mechanism for the case of  $N_r$  receive antennas.

1) *Description*: As mentioned earlier, Alamouti STBC uses two transmit antennas regardless of the number of receive antennas. The Alamouti scheme encoding operation is given by (8). In this paper, the rows of each coding scheme represents a different time instant, while the columns represent the transmitted symbol through each different antenna. In this case, the first and second row represent the transmission at the first and second time instant respectively. At a time  $t$ , the symbol  $s_1$  and symbol  $s_2$  are transmitted from antenna 1 and antenna 2 respectively. Assuming that each symbol has duration  $T$ , then at time  $t + T$ , the symbols  $-s_2^*$  and  $s_1^*$ , where  $(\cdot)^*$  denotes the complex conjugate, are transmitted from antenna 1 and antenna 2 respectively.

$$\mathcal{G}_2 = \begin{pmatrix} s_1 & s_2 \\ -s_2^* & s_1^* \end{pmatrix} \quad (8)$$

2) *Case of 1 Receive Antenna*: The reception and decoding of the signal depends on the number of receive antennas available. For the case of one receive antenna, the receive signals are [14]:

$$\begin{aligned} r_1^{(1)} &= r_1(t) = h_{1,1}s_1 + h_{1,2}s_2 + n_1^{(1)} \\ r_1^{(2)} &= r_1(t+T) = -h_{1,1}s_2^* + h_{1,2}s_1^* + n_1^{(2)} \end{aligned} \quad (9)$$

where  $r_1$  is the received signal at antenna 1,  $h_{i,j}$  is the channel transfer function from the  $j^{\text{th}}$  transmit antenna and the  $i^{\text{th}}$  receive antenna defined in Section II,  $n_1$  is a complex random variable representing noise at antenna 1, and  $x^{(\kappa)}$  denotes  $x$  at time instant  $\kappa$  (i.e. at time  $t + (\kappa - 1)T$ ).

Before the received signals are sent to the decoder, they are combined as follows [14]:

$$\begin{aligned} \tilde{s}_1 &= h_{1,1}^* r_1^{(1)} + h_{1,2} r_1^{*(2)} \\ \tilde{s}_2 &= h_{1,2}^* r_1^{(1)} + h_{1,1} r_1^{*(2)} \end{aligned} \quad (10)$$

and substituting (9) in (10) yields:

$$\begin{aligned} \tilde{s}_1 &= (\alpha_{1,1}^2 + \alpha_{1,2}^2) s_1 + h_{1,1}^* n_1^{(1)} + h_{1,2} n_1^{*(2)} \\ \tilde{s}_2 &= (\alpha_{1,1}^2 + \alpha_{1,2}^2) s_2 - h_{1,1} n_1^{*(2)} + h_{1,2}^* n_1^{(1)} \end{aligned} \quad (11)$$

where  $\alpha_{i,j}^2$  is the squared magnitude of the channel transfer function  $h_{i,j}$ . The calculated  $\tilde{s}_1$  and  $\tilde{s}_2$  are then sent to a Maximum Likelihood (ML) decoder to estimate the transmitted symbols  $s_1$  and  $s_2$  respectively [14].

3) *Case of 2 Receive Antennas:* For the case of two receive antennas, the received symbols are [14]:

$$\begin{aligned} r_1^{(1)} &= h_{1,1}s_1 + h_{1,2}s_2 + n_1^{(1)} \\ r_1^{(2)} &= -h_{1,1}s_2^* + h_{1,2}s_1^* + n_1^{(2)} \\ r_2^{(1)} &= h_{2,1}s_1 + h_{2,2}s_2 + n_2^{(1)} \\ r_2^{(2)} &= -h_{2,1}s_2^* + h_{2,2}s_1^* + n_2^{(2)} \end{aligned} \quad (12)$$

and the combined signals are [14]:

$$\begin{aligned} \tilde{s}_1 &= h_{1,1}^*r_1^{(1)} + h_{1,2}r_1^{*(2)} + h_{2,1}^*r_2^{(1)} + h_{2,2}r_2^{*(2)} \\ \tilde{s}_2 &= h_{1,2}^*r_1^{(1)} + h_{1,1}r_1^{*(2)} + h_{2,2}^*r_2^{(1)} + h_{2,1}r_2^{*(2)} \end{aligned} \quad (13)$$

which, after substituting (12) becomes:

$$\begin{aligned} \tilde{s}_1 &= (\alpha_{1,1}^2 + \alpha_{1,2}^2 + \alpha_{2,1}^2 + \alpha_{2,2}^2)s_1 \\ &\quad + h_{1,1}^*n_1^{(1)} + h_{1,2}n_1^{*(2)} + h_{2,1}^*n_2^{(1)} + h_{2,2}n_2^{*(2)} \\ \tilde{s}_2 &= (\alpha_{1,1}^2 + \alpha_{1,2}^2 + \alpha_{2,1}^2 + \alpha_{2,2}^2)s_2 \\ &\quad - h_{1,1}n_1^{*(2)} + h_{1,2}^*n_1^{(1)} - h_{2,1}n_2^{*(2)} + h_{2,2}^*n_2^{(1)} \end{aligned} \quad (14)$$

4) *Decoding decision statistic for  $N_r$  receive antennas:*

The ML decoder decision statistic decodes in favor of  $s_1$  and  $s_2$  over all possible values of  $s_1$  and  $s_2$  such that (15) and (16) are minimized where  $\psi$  is given by (17) for  $N_t = 2$  [15], [11].

$$\left| \left[ \sum_{i=1}^{N_r} (r_i^{(1)}h_{i,1}^* + r_i^{*(2)}h_{i,2}) \right] - s_1 \right|^2 + \psi|s_1|^2 \quad (15)$$

$$\left| \left[ \sum_{i=1}^{N_r} (r_i^{(1)}h_{i,2}^* - r_i^{*(2)}h_{i,1}) \right] - s_2 \right|^2 + \psi|s_2|^2 \quad (16)$$

$$\psi = \left( -1 + \sum_{i=1}^{N_r} \sum_{j=1}^{N_t} |h_{i,j}|^2 \right) \quad (17)$$

Alamouti STBC does not require CSI at the transmitter. Also, the Alamouti STBC can be used with 2 transmit antennas and 1 receive antenna while accomplishing the full diversity of 2. This is an important characteristic of Alamouti STBC as it reduces the effect of fading at mobile stations while only requiring extra antenna elements at the base station, where it is more economical than having multiple antennas at the receivers [14]. However, if having more antennas at the receivers is not a problem, this scheme can be used with 2 transmit antennas and  $N_r$  receive antennas while accomplishing a  $2N_r$  full diversity. The case space time block codes for  $N_t > 2$  is discussed in the following section.

### B. Orthogonal Space-Time Block Codes

The Alamouti scheme discussed in Section III-A is part of a general class of STBCs known as Orthogonal Space-Time

Block Codes (OSTBCs) [4]. The authors of [15] apply the mathematical framework of orthogonal designs to construct both real and complex orthogonal codes that achieve full diversity. For the case of real orthogonal codes, it has been shown that a full rate code can be constructed [15]. However, for the case of complex orthogonal codes, it is unknown if a full rate and full diversity codes exist for  $N_t > 2$  [3]. Complex modulation techniques are of interest in this paper and therefore real orthogonal codes are not discussed. In next sections, the full diversity complex orthogonal codes presented in [15] for different rates are briefly introduced.

1) *Orthogonal Space-Time Block Codes for  $N_t = 3$ :* For the case of 3 transmit antennas, Tarokh et al. construct block codes for the with 1/2 and 3/4 coding rate and full diversity  $3N_r$ .

a)  *$N_t = 3$  with Rate 1/2:* The full diversity, rate 1/2 code for  $N_t = 3$  is given by [15], [11]:

$$\mathcal{G}_3 = \begin{pmatrix} s_1 & s_2 & s_3 \\ -s_2 & s_1 & -s_4 \\ -s_3 & s_4 & s_1 \\ -s_4 & -s_3 & s_2 \\ s_1^* & s_2^* & s_3^* \\ -s_2^* & s_1^* & -s_4^* \\ -s_3^* & s_4^* & s_1^* \\ -s_4^* & -s_3^* & s_2^* \end{pmatrix} \quad (18)$$

This code transmits 4 symbols every 8 time intervals, and therefore has rate 1/2. The decision metric to minimize by the decoder for detecting  $s_1, s_2, s_3, s_4$  are given by (20), (21), (22), (23) respectively where

$$\xi = \left( -1 + 2 \sum_{i=1}^{N_r} \sum_{j=1}^{N_t} |h_{i,j}|^2 \right) \quad (19)$$

for  $N_t = 3$  [11].

$$\begin{aligned} &\left| \left[ \sum_{i=1}^{N_r} (r_i^{(1)}h_{i,1}^* + r_i^{(2)}h_{i,2}^* + r_i^{(3)}h_{i,3}^* \right. \right. \\ &\quad \left. \left. + r_i^{*(5)}h_{i,1} + r_i^{*(6)}h_{i,2} + r_i^{*(7)}h_{i,3}) \right] - s_1 \right|^2 \\ &\quad + \xi|s_1|^2 \end{aligned} \quad (20)$$

$$\begin{aligned} &\left| \left[ \sum_{i=1}^{N_r} (r_i^{(1)}h_{i,2}^* - r_i^{(2)}h_{i,1}^* + r_i^{(4)}h_{i,3}^* \right. \right. \\ &\quad \left. \left. + r_i^{*(5)}h_{i,2} - r_i^{*(6)}h_{i,1} + r_i^{*(8)}h_{i,3}) \right] - s_2 \right|^2 \\ &\quad + \xi|s_2|^2 \end{aligned} \quad (21)$$

$$\left[ \left[ \sum_{i=1}^{N_r} (r_i^{(1)} h_{i,3}^* - r_i^{(3)} h_{i,1}^* - r_i^{(4)} h_{i,2}^* + r_i^{*(5)} h_{i,3} - r_i^{*(7)} h_{i,1} - r_i^{*(8)} h_{i,2}) \right] - s_3 \right]^2 + \xi |s_3|^2 \quad (22)$$

$$\left[ \left[ \sum_{i=1}^{N_r} (-r_i^{(2)} h_{i,3}^* + r_i^{(3)} h_{i,2}^* - r_i^{(4)} h_{i,1}^* - r_i^{*(6)} h_{i,3} + r_i^{*(7)} h_{i,2} - r_i^{*(8)} h_{i,1}) \right] - s_4 \right]^2 + \xi |s_4|^2 \quad (23)$$

b)  $N_t = 3$  with Rate 3/4: A higher rate code with  $N_t = 3$  is given by [15], [11]:

$$\mathcal{H}_3 = \begin{pmatrix} s_1 & s_2 & \frac{s_3}{\sqrt{2}} \\ -s_2^* & s_1^* & \frac{s_3}{\sqrt{2}} \\ \frac{s_3}{\sqrt{2}} & \frac{s_3}{\sqrt{2}} & \frac{-s_1 - s_1^* + s_2 - s_2^*}{2} \\ \frac{s_3}{\sqrt{2}} & -\frac{s_3}{\sqrt{2}} & \frac{s_2 + s_2^* + s_1 - s_1^*}{2} \end{pmatrix} \quad (24)$$

As can be observed, (24) transmits 3 symbols every 4 time intervals, and therefore has rate 3/4. The decision statistic to minimize for detecting  $s_1$ ,  $s_2$ , and  $s_3$  are given by (25), (26), and (27) respectively

$$\left[ \left[ \sum_{i=1}^{N_r} \left( r_i^{(1)} h_{i,1}^* + r_i^{*(2)} h_{i,2} + \frac{(r_i^{(4)} - r_i^{(3)}) h_{i,3}^*}{2} - \frac{(r_i^{(3)} + r_i^{(4)})^* h_{i,3}}{2} \right) \right] - s_1 \right]^2 + \psi |s_1|^2 \quad (25)$$

$$\left[ \left[ \sum_{i=1}^{N_r} \left( r_i^{(1)} h_{i,2}^* - r_i^{*(2)} h_{i,1} + \frac{(r_i^{(4)} + r_i^{(3)}) h_{i,3}^*}{2} + \frac{(-r_i^{(3)} + r_i^{(4)})^* h_{i,3}}{2} \right) \right] - s_2 \right]^2 + \psi |s_2|^2 \quad (26)$$

$$\left[ \left[ \sum_{i=1}^{N_r} \left( \frac{(r_i^{(1)} + r_i^{(2)}) h_{i,3}^*}{\sqrt{2}} + \frac{r_i^{*(3)} (h_{i,1} + h_{i,2})}{\sqrt{2}} + \frac{r_i^{*(4)} (h_{i,1} - h_{i,2})}{\sqrt{2}} \right) \right] - s_3 \right]^2 + \psi |s_3|^2 \quad (27)$$

2) *Orthogonal Space-Time Block Codes for  $N_t = 4$* : For the case of 4 transmit antennas, [15] provide block codes of rate 1/2 and 3/4, both of which have full diversity  $4N_r$ .

a)  $N_t = 4$  with Rate 1/2: In the case of 4 transmit antennas, the rate 1/2 code block is given by [15], [11]:

$$\mathcal{G}_4 = \begin{pmatrix} s_1 & s_2 & s_3 & s_4 \\ -s_2 & s_1 & -s_4 & s_3 \\ -s_3 & s_4 & s_1 & -s_2 \\ -s_4 & -s_3 & s_2 & s_1 \\ s_1^* & s_2^* & s_3^* & s_4^* \\ -s_2^* & s_1^* & -s_4^* & s_3^* \\ -s_3^* & s_4^* & s_1^* & -s_2^* \\ -s_4^* & -s_3^* & s_2^* & s_1^* \end{pmatrix} \quad (28)$$

where, similar to (18), has rate 1/2 as 4 symbols are transmitted in 8 time intervals. To decode, the ML decoder minimizes the decision metric (29), (30), (31), and (32) for decoding  $s_1$ ,  $s_2$ ,  $s_3$ , and  $s_4$  respectively where  $\xi$  is given by (19) for  $N_t = 4$  [11]. The decoding decision metric (32) for decoding  $s_4$  differs from that of [11] since the author discovered a mistake in the metric provided by Tarokh et al.

$$\left[ \left[ \sum_{i=1}^{N_r} (r_i^{(1)} h_{i,1}^* + r_i^{(2)} h_{i,2}^* + r_i^{(3)} h_{i,3}^* + r_i^{(4)} h_{i,4}^* + r_i^{*(5)} h_{i,1} + r_i^{*(6)} h_{i,2} + r_i^{*(7)} h_{i,3} + r_i^{*(8)} h_{i,4}) \right] - s_1 \right]^2 + \xi |s_1|^2 \quad (29)$$

$$\left[ \left[ \sum_{i=1}^{N_r} (r_i^{(1)} h_{i,2}^* - r_i^{(2)} h_{i,1}^* - r_i^{(3)} h_{i,4}^* + r_i^{(4)} h_{i,3}^* + r_i^{*(5)} h_{i,2} - r_i^{*(6)} h_{i,1} - r_i^{*(7)} h_{i,4} + r_i^{*(8)} h_{i,3}) \right] - s_2 \right]^2 + \xi |s_2|^2 \quad (30)$$

$$\left[ \left[ \sum_{i=1}^{N_r} (r_i^{(1)} h_{i,3}^* + r_i^{(2)} h_{i,4}^* - r_i^{(3)} h_{i,1}^* - r_i^{(4)} h_{i,2}^* + r_i^{*(5)} h_{i,3} + r_i^{*(6)} h_{i,4} - r_i^{*(7)} h_{i,1} - r_i^{*(8)} h_{i,2}) \right] - s_3 \right]^2 + \xi |s_3|^2 \quad (31)$$

$$\left[ \left[ \sum_{i=1}^{N_r} (r_i^{(1)} h_{i,4}^* - r_i^{(2)} h_{i,3}^* + r_i^{(3)} h_{i,2}^* - r_i^{(4)} h_{i,1}^* + r_i^{*(5)} h_{i,4} - r_i^{*(6)} h_{i,3} + r_i^{*(7)} h_{i,2} - r_i^{*(8)} h_{i,1}) \right] - s_4 \right]^2 + \xi |s_4|^2 \quad (32)$$

b)  $N_t = 4$  with Rate 3/4: A 4 transmit antenna block code with rate 3/4 is given by [15], [11]:

$$\mathcal{H}_4 = \begin{pmatrix} s_1 & s_2 & \frac{s_3}{\sqrt{2}} & \frac{s_3}{\sqrt{2}} \\ -s_2^* & s_1^* & \frac{s_3}{\sqrt{2}} & -\frac{s_3}{\sqrt{2}} \\ \frac{s_2^*}{\sqrt{2}} & \frac{s_1^*}{\sqrt{2}} & \frac{-s_1-s_1^*+s_2-s_2^*}{2} & \frac{-s_2-s_2^*+s_1-s_1^*}{2} \\ \frac{s_3^*}{\sqrt{2}} & -\frac{s_3^*}{\sqrt{2}} & \frac{s_2+s_2^*+s_1-s_1^*}{2} & \frac{-s_1+s_1^*+s_2-s_2^*}{2} \end{pmatrix} \quad (33)$$

The decision metrics to minimize for decoding  $s_1$ ,  $s_2$ , and  $s_3$  are given by (34), (35), and (36) respectively.

$$\left| \left[ \sum_{i=1}^{N_r} \left( r_i^{(1)} h_{i,1}^* + r_i^{*(2)} h_{i,2} + \frac{(r_i^{(4)} - r_i^{(3)})(h_{i,3}^* - h_{i,4}^*)}{2} - \frac{(r_i^{(3)} + r_i^{(4)})^*(h_{i,3} + h_{i,4})}{2} \right) \right] - s_1 \right|^2 + \psi |s_1|^2 \quad (34)$$

$$\left| \left[ \sum_{i=1}^{N_r} \left( r_i^{(1)} h_{i,2}^* - r_i^{*(2)} h_{i,1} + \frac{(r_i^{(4)} + r_i^{(3)})(h_{i,3}^* - h_{i,4}^*)}{2} + \frac{(-r_i^{(3)} + r_i^{(4)})^*(h_{i,3} + h_{i,4})}{2} \right) \right] - s_2 \right|^2 + \psi |s_2|^2 \quad (35)$$

$$\left| \left[ \sum_{i=1}^{N_r} \left( \frac{(r_i^{(1)} + r_i^{(2)}) h_{i,3}^*}{\sqrt{2}} + \frac{(r_i^{(1)} - r_i^{(2)}) h_{i,4}}{\sqrt{2}} + \frac{r_i^{*(3)}(h_{i,1} + h_{i,2})}{\sqrt{2}} + \frac{r_i^{*(4)}(h_{i,1} - h_{i,2})}{\sqrt{2}} \right) \right] - s_3 \right|^2 + \psi |s_3|^2 \quad (36)$$

Now that the block codes and their decoding metrics have been presented, the simulation setup is discussed, followed by results and analysis, and finally the conclusion.

#### IV. SIMULATIONS

Simulations are done in MATLAB using the Rayleigh channel model described in Section II-B1. We simulate  $\mathcal{G}_2$ ,  $\mathcal{G}_3$ ,  $\mathcal{G}_4$ ,  $\mathcal{H}_3$ , and  $\mathcal{H}_4$ , for the case of  $N_r = 1$  up to  $N_r = 4$ . We modulate using BPSK, QPSK, 4-QAM, 16-QAM, and 64-QAM gray mapping constellations. For each sample, blocks of  $10^4$  symbols are simulated until at least 100 bit errors are obtained, or until  $10^4$  blocks are simulated. The simulation is stopped when the SNR reached 40dB or after simulating  $10^4$  blocks without errors. Consequently, each value obtained for the bit-error rate (BER) of  $10^{-7}$  with 100 errors has a 99.9% confidence level. Both the MATLAB simulation source code and the data collected from the simulations are available at [16].

#### V. RESULTS AND ANALYSIS

Keeping all other variables the same, the results obtained for BPSK and QPSK are nearly identical, and we therefore present data for QPSK and omit that of BPSK. Since the data is nearly

identical, the reader can safely assume that the performance of BPSK is that of QPSK. We study the performance of each block code discussed earlier for the different cases of constant  $N_r$ ,  $N_t$ , rate, and diversity order.

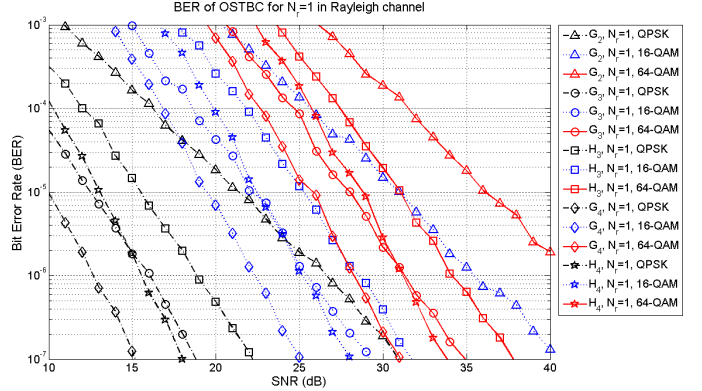


Fig. 2. Bit error rate versus SNR of OSTBC for  $N_r = 1$ .

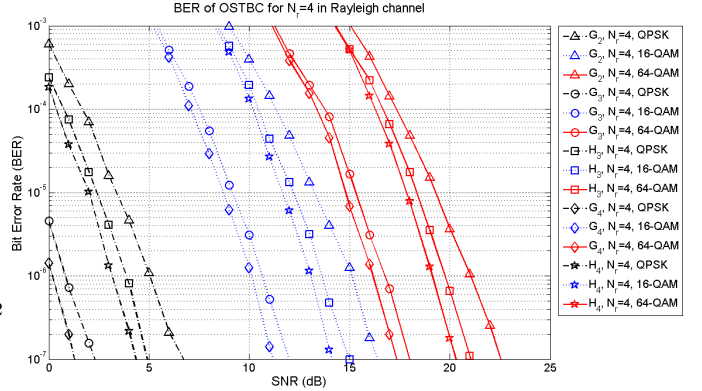
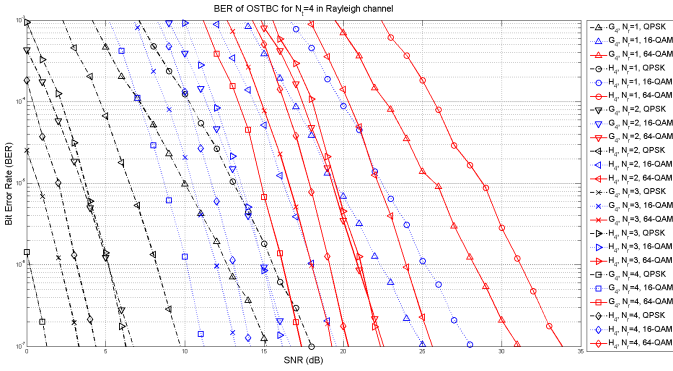


Fig. 3. Bit error rate versus SNR of OSTBC for  $N_r = 4$ .

For the case of  $N_r$  constant, we fix  $N_r = 1$ . The result is shown in Figure 2. As expected, for each different code blocks, the performance degrades as more bits per symbol are transmitted. It can be observed that for a particular modulation and high SNR, the best performance is obtained by  $\mathcal{G}_4$  followed by  $\mathcal{H}_4$ ,  $\mathcal{G}_3$ ,  $\mathcal{H}_3$ , and  $\mathcal{G}_2$ . However, for any modulation and low SNR,  $\mathcal{G}_3$  outperforms  $\mathcal{H}_4$  even when  $\mathcal{H}_4$  has greater gain. The results is that the best performance at low SNR is obtained by  $\mathcal{G}_4$  followed by  $\mathcal{G}_3$ ,  $\mathcal{H}_4$ ,  $\mathcal{H}_3$ , and  $\mathcal{G}_2$ . Moreover,  $\mathcal{H}_4$  is outperformed by  $\mathcal{G}_3$  for the cases of  $N_r = 2$ ,  $N_r = 3$ , and  $N_r = 4$ .

Figure 3 shows the case where  $N_r$  is fixed to 4. As can be observed, for a particular modulation, the best performance is obtained by  $\mathcal{G}_4$  followed by  $\mathcal{G}_3$ ,  $\mathcal{H}_4$ ,  $\mathcal{H}_3$ , and  $\mathcal{G}_2$ . This order is the same as for the case of  $N_r = 1$  and low SNR where  $\mathcal{G}_3$  outperforms  $\mathcal{H}_4$  even with  $\mathcal{H}_4$  having higher gain. One possible reason for this behaviour is that the higher rate of  $\mathcal{H}_4$  causes lower channel gain per symbol and therefore higher BER for a particular SNR.

The BER curve for the case of keeping  $N_t = 4$  constant while varying  $N_r$  from 1 to 4 for different modulations

Fig. 4. Bit error rate versus SNR of OSTBC for  $N_t = 4$ .

is depicted in Figure 4. It can be observed that for any modulation and block code, the gain of using 3 more antennas is approximately  $14dB$ . However, between  $N_r = 1$  and  $N_r = 2$  the gain is approximately  $8dB$ , between  $N_r = 2$  and  $N_r = 3$  the gain is approximately  $4dB$ , and between  $N_r = 3$  and  $N_r = 4$  the gain is approximately  $2dB$ . This result suggest diminishing returns as  $N_r$  increases. Another observation is that for any  $N_r$  and modulation scheme,  $\mathcal{G}_3$  and  $\mathcal{G}_4$  have a  $3dB$  gain over  $\mathcal{H}_3$  and  $\mathcal{H}_4$  respectively. An interesting observation is that the performance of  $\mathcal{G}_4$  with  $N_r = 2$  is similar to that of  $\mathcal{H}_4$  with  $N_r = 3$ , while  $\mathcal{G}_4$  with  $N_r = 1$  is outperformed by  $\mathcal{H}_4$  with  $N_r = 2$ , and  $\mathcal{G}_4$  with  $N_r = 3$  outperforms  $\mathcal{H}_4$  with  $N_r = 4$ .

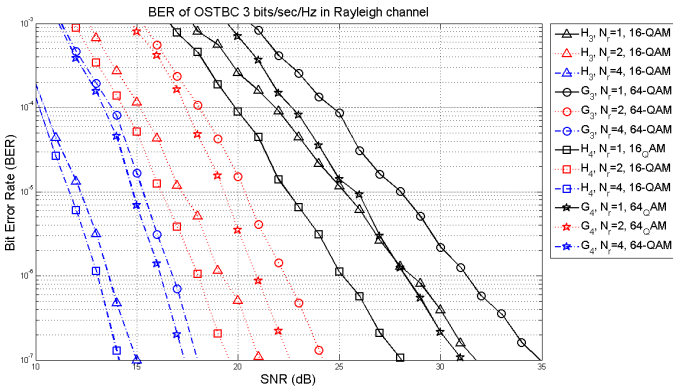


Fig. 5. Bit error rate versus SNR of OSTBC at 3 bits/sec/Hz.

In order to fairly compare all the block code schemes, a comparison with equal data rate and a comparison with equal diversity gain is needed. For the case of equal data rate, we simulate  $\mathcal{H}_3$  and  $\mathcal{H}_4$  with constellation 16-QAM, and  $\mathcal{G}_3$  and  $\mathcal{G}_4$  with constellation 64-QAM. Since  $\mathcal{H}_3$  and  $\mathcal{H}_4$  have code rate  $3/4$ , using 16-QAM (4 bits/symbol) leads to 3 bits/sec/Hz. Similarly, since  $\mathcal{G}_3$  and  $\mathcal{G}_4$  have code rate  $1/2$ , using 64-QAM (6 bits/symbol) leads to 3 bits/sec/Hz. The result for  $N_r = 1$ ,  $N_r = 2$ , and  $N_r = 4$  is presented in Figure 5. As expected, having more receive diversity leads to better performance on all cases. In general, there is a  $3dB$  gain when using the 16-QAM lower order constellations with higher code rate  $3/4$  over using the 64-QAM higher order constellation with lower

code rate  $1/2$  for the same number of transmit antennas. It is particularly interesting to notice that at high SNR and  $N_r = 1$ , 64-QAM  $\mathcal{G}_4$  outperforms 16-QAM  $\mathcal{H}_3$  while at low SNR and  $N_r = 1$ , 16-QAM  $\mathcal{H}_3$  outperforms 64-QAM  $\mathcal{G}_4$ .

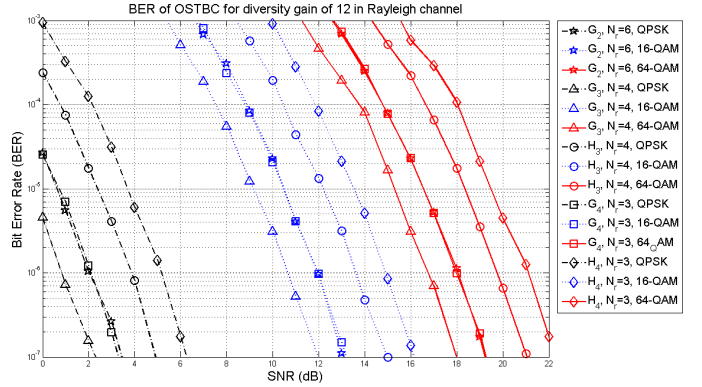


Fig. 6. Bit error rate versus SNR of OSTBC with spatial diversity 12.

Figure 6 displays a BER curve for the case of equal diversity gain. To accomplish this, we simulate  $\mathcal{G}_2$  with  $N_r = 6$ ,  $\mathcal{G}_3$  and  $\mathcal{H}_3$  with  $N_r = 4$ , and  $\mathcal{G}_4$  and  $\mathcal{H}_4$  with  $N_r = 3$ . The diversity gain in each case is therefore 12. From Figure 6 we see that having fewer number of transmit antennas and more number of receive antennas results in better performance.  $\mathcal{G}_3$  and  $\mathcal{H}_3$  with  $N_r = 4$  have a  $2dB$  performance gain over  $\mathcal{G}_4$  and  $\mathcal{G}_4$  with  $N_r = 3$  respectively. This result agrees with [14] since (1) must hold true which says that as the number of transmit antennas increase, the energy per transmit antenna decreases. It is also interesting to see that  $\mathcal{G}_2$  with  $N_r = 6$  has similar performance as to  $\mathcal{G}_4$  with  $N_r = 3$ . This observation suggests that there is an upper limit at which using few  $N_t$  transmit antennas and more  $N_r$  receive antennas becomes equivalent to using more  $N_t$  transmit antennas and fewer  $N_r$  receive antennas. This is important since, as previously mentioned, it is more economical to increase the number of  $N_t$  transmit antennas at the base station than increasing the number of  $N_r$  receive antennas at all mobile stations.

## VI. CONCLUSION

This paper provided a basic overview of MIMO systems. We briefly discussed MIMO channel modeling techniques. A basic introduction to Space-Time Coding was provided by presenting Alamouti's scheme. We then discussed block codes schemes with different code rates for the cases of 3 and 4 transmit antennas. The encoding and decoding algorithms for each were both presented. For the case of  $\mathcal{G}_4$ , the decoding metric of  $s_4$  was corrected from the original publication presented by Tarokh et al. Simulation results were then presented. It was observed that higher diversity gain does not always imply better performance. This was observed when  $\mathcal{G}_3$  outperformed  $\mathcal{H}_4$  at low SNR for  $N_r = 1$  and at any SNR for  $N_r = 2$  up to  $N_r = 4$ . Similarly, it was observed that equal diversity gain does not imply equal performance. This was particularly demonstrated when  $\mathcal{G}_3$  outperformed all others for equal diversity gain. The penalty of having more

transmit antennas, which consequently reduces the energy per transmit antenna was observed. Also, we observed diminishing returns for every scheme as the number of received antennas increased. It was particularly interesting to find that although  $\mathcal{H}_3$  and  $\mathcal{H}_4$  have higher rate than  $\mathcal{G}_3$  and  $\mathcal{G}_4$ , the performance of  $\mathcal{G}_3$  and  $\mathcal{G}_4$  is greater and could therefore be preferred in some scenarios. Finally, we conclude that it is preferable to use a low constellation order with high code rate than high constellation order with low code rate.

#### REFERENCES

- [1] A. Molisch, *Wireless Communications*. Wiley-IEEE Press, 2005.
- [2] J. Winters, "On the capacity of radio communication systems with diversity in a Rayleigh fading environment," *IEEE Journal on Selected Areas in Communications*, vol. 5, no. 5, pp. 871–878, 1987.
- [3] D. Gesbert, M. Shafi, D. Shiu, P. Smith, and A. Naguib, "From theory to practice: an overview of MIMO space-time coded wireless systems," *IEEE Journal on selected areas in Communications*, vol. 21, no. 3, pp. 281–302, 2003.
- [4] G. Tsoulos, *MIMO system technology for wireless communications*. CRC Press, 2006.
- [5] L. Dai, S. Zhou, H. Zhuang, and Y. Yao, "Closed-loop MIMO architecture based on water-filling," *Electronics Letters*, vol. 38, no. 25, pp. 1718–1720, 2002.
- [6] K. Zheng, L. Huang, W. Wang, and G. Yang, "TD-CDM-OFDM: Evolution of TD-SCDMA toward 4G," *IEEE Communications Magazine*, vol. 43, no. 1, pp. 45–52, 2005.
- [7] H. Sampath, S. Talwar, J. Tellado, V. Erceg, and A. Paulraj, "A fourth-generation MIMO-OFDM broadband wireless system: design, performance, and field trial results," *IEEE Communications Magazine*, vol. 40, no. 9, pp. 143–149, 2002.
- [8] "IEEE P802.11n/D5.0," May 2008.
- [9] H. Niu and Ngo, "Diversity and Multiplexing Switching in 802.11 n MIMO Systems," in *Signals, Systems and Computers, 2006. ACSSC'06. Fortieth Asilomar Conference on*, 2006, pp. 1644–1648.
- [10] G. Foschini and M. Gans, "On limits of wireless communications in a fading environment when using multiple antennas," *Wireless personal communications*, vol. 6, no. 3, pp. 311–335, 1998.
- [11] V. Tarokh, H. Jafarkhani, and A. Calderbank, "Space-time block coding for wireless communications: performance results," *IEEE Journal on selected areas in communications*, vol. 17, no. 3, pp. 451–460, 1999.
- [12] T. Kaiser, *Smart Antennas—State of the Art*. Hindawi Publishing Corporation, 2005.
- [13] A. Molisch, "A generic model for MIMO wireless propagation channels in macro-and microcells," *IEEE Transactions on Signal Processing*, vol. 52, no. 1, pp. 61–71, 2004.
- [14] S. Alamouti, "A simple transmit diversity technique for wireless communications," *IEEE Journal on selected areas in communications*, vol. 16, no. 8, pp. 1451–1458, 1998.
- [15] V. Tarokh, H. Jafarkhani, and A. Calderbank, "Space-time block codes from orthogonal designs," *IEEE Transactions on Information Theory*, vol. 45, no. 5, pp. 1456–1467, 1999.
- [16] L. Cortes-Pena, "Orthogonal Space-Time Coding Matlab Source Files," *Software on-line*: [http://users.ece.gatech.edu/~cortes/STBC\\_Matlab.html](http://users.ece.gatech.edu/~cortes/STBC_Matlab.html), 2009.